GRAVITY-DRIVEN CONVECTIVE FLOW OF MAGNETITE-WATER NANOFLUID AND RADIATIVE HEAT TRANSFER PAST AN OSCILLATING VERTICAL PLATE IN THE PRESENCE OF MAGNETIC FIELD

G.S. SETH† and P.K. MANDAL‡

Department of Applied Mathematics, Indian Institute of Technology (Indian School of Mines), Dhanbad - 826004, India
† gsseth_ism@yahoo.com (Corresponding author)
‡ ism.prashanta@gmail.com

***Abstract*— This study investigates heat transfer in magnetohydrodynamic (MHD) free convection flow of ferrofluid along an oscillating vertical plate. Water with nanoparticles of magnetite (Fe_3O_4) is selected as a conventional base fluid. In addition, non-magnetic aluminum oxide (Al_2O_3) nanoparticles are also used. Comparison between magnetic (Fe_3O_4) and non-magnetic (Al_2O_3) nanoparticles is also conducted. The problem was modelled in terms of partial differential equations with the initial and boundary conditions. Analytical solutions are obtained for velocity and temperature by using Laplace transform technique. The numerical results for velocity and temperature are obtained and plotted graphically. Also numerical values of skin friction and Nusselt number are presented in tables and discussed.**

***Keywords*— Ferrofluid, Free convection, Magnetic field, Ramped wall temperature.**

I. INTRODUCTION

In modern thermal and manufacturing processes, the influences of working fluids depend on thermal conductivity, heat capacity and other physical properties. Potential for heat transfer in the high-tech applications such as microelectronics, data centers and micro-channels have given most attentions in the recent past. Conventional heat transfer fluids such as ethylene glycol, water, pumping oil, etc., do not possess sufficient capability for cooling applications due to their poor thermal performance. It is well known that solid metals have thermal conductivities of higher order of magnitude than those of fluids. Thus one of effective approaches to enhance heat transfer performance is via adding small metallic particle in the liquids. The idea of improving thermal conductivity of the fluid using nano-sized particles was initially initiated by Choi (1995). Base fluids with the mixture of nanoparticles are termed as nanofluids. In nano particles due to the increase of surface area to the volume, some physical properties such as thermal, electrical, mechanical, optical and magnetic property of the materials can be changed significantly.

Convective flows with radiation are encountered in many industrial processes such as heating and cooling of chambers, evaporation from large reservoirs, solar power technology and space vehicle re-entry. The study of magneto hydrodynamic flow and heat transfer has received considerable attention in recent years due to its essential applications in engineering and technology such as MHD generators, pumps, plasma studies, bearings, nuclear reactors and geothermal energy extractions. The gravity-driven convection heat transfer is important in the cooling mechanism of many engineering systems like the electronics industry, solar collectors and cooling systems for nuclear reactors because of its smaller size, low noise, minimum cost and reliability. Sheikholeslami *et al*. (2013) investigated the MHD effects on Al_2O_3 - water nanofluid flow and heat transfer in a semi-annulus enclosure using Lattice Boltzmann Method. Kuznetsov and Nield (2014) analysed the natural convective boundary layer flow of a nanofluid past a vertical plate. Mutuku-Njane and Makinde (2014) considered hydromagnetic boundary layer flow of nanofluids over a permeable moving surface with Newtonian heating. Beg *et al*. (2014) conducted a computational fluid dynamics simulation of laminar convection of Al_2O_3 –water bio-nanofluids in a circular tube under constant wall temperature conditions considering a single-phase model and three different two-phase models. Das and Jana (2015) investigated natural convective magneto-nanofluid flow and radiative heat transfer past a moving vertical plate. Relevant studies on nanofluid flow considering different aspects of the problems are also due to Khamis *et al*. (2015), Das *et al*. (2015) and Bhatti and Rashidi (2016).

An electrically conducting nanofluid known as ferrofluid, is a magnetic colloidal suspension consisting of base liquid and magnetic (iron based) nanoparticles such as magnetite, hematite, cobalt ferrite or some other compounds containing iron, with a size range of 5-15 nm in diameter coated with a surfactant layer. Ferrofluids have an advantage, which is based on the control of fluid flow and heat transfer by an external magnetic field, which makes it applicable in various fields such as electronic packing, thermal, aerospace and biomedical engineerings. Ferrofluids are widely used in rotating X-ray tubes, sealing of hard disc drives and underwater robotic vehicle under engineering applications. Keeping in view importance of such study, several researchers have investigated ferrofluid flow under different conditions and configurations. A few relevant studies are due to Jue (2006), Khan *et al*. (2014), Sheikholeslami and Ganji (2014), Moraveji and Hejazian (2013), Gul *et al*. (2015), Sheikholeslami *et al*. (2015) and Mustafa *et al*. (2016).

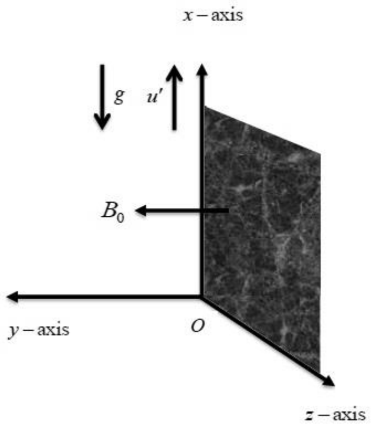

Figure 1: Schematic diagram of the physical problem.

A number of investigations were implemented under different type of continuous and well-defined thermal conditions at the wall. However, practical problems often involve non-uniform or arbitrary wall conditions. Thus, it is useful to investigate problems considering step change in wall temperature. Pioneering works are due to Schetz (1963), Lee and Yovanovich (1991), Chandran *et al*. (2005), Nandkeolyar *et al*. (2013), Khalid *et al*. (2015) and Seth *et al*. (2011). Adesanya *et al*. (2015) described hydromagnetic natural convection flow within vertical parallel plate channel with time periodic boundary conditions. Rashidi *et al*. (2016) investigated mixed convection heat transfer of nanofluid flow in vertical channel with sinusoidal walls under magnetic field effect.

Motivated by the above research works and the numerous possible industrial applications, the present paper is aimed to investigate the free convective flow of ferrofluid past an infinite oscillating vertical plate with ramped wall temperature in the presence of magnetic field and thermal radiation.

II. MATHEMATICAL FORMULATION OF THE PROBLEM

We consider unsteady gravity-driven convective flow and heat transfer of an optically thin water-based nanofluid containing magnetite (Fe_3O_4) nanoparticles past an oscillating infinite vertical plate. The fluid flow is permeated with uniform magnetic field of strength B_0, applied in a transverse direction to the flow. It is assumed that there exists a radiative heat flux q_r acting in the normal direction of the plate whereas radiative heat flux along the plate is considered as negligible. The schematic diagram of the physical problem is presented in Fig. 1.

The induced magnetic field produced by the fluid motion is negligible under the assumption of a small magnetic Reynolds number.

Keeping in view the assumptions made above, the momentum and energy equations under Bossinesq's approximations (Das and Jana, 2015; Khalid *et al*., 2015) are given by

$$\rho_{nf}\frac{\partial u'}{\partial t'}=\mu_{nf}\frac{\partial^2 u'}{\partial y^2}+g\left(\rho\beta\right)_{nf}\left(T-T_\infty\right)-\sigma_{nf}B_0^2u', \quad (1)$$

Table 1: Thermo-physical properties of water and nanoparticles (Sheikholeslami *et al*., 2014; 2015).

	ρ(kg/m^3)	C_p(J/kgK)	k(W/mK)	$\beta\times10^5$(K^{-1})	$\sigma(\Omega\text{m})^{-1}$
Pure water	997.1	4179	0.613	21	0.05
Fe_3O_4	5200	670	6	1.3	25000
Al_2O_3	3970	765	40	0.85	1×10^{-10}

$$\left(\rho C_p\right)_{nf}\frac{\partial T}{\partial t}=k_{nf}\frac{\partial^2 T}{\partial y^2}-\frac{\partial q_r}{\partial y}, \quad (2)$$

The initial and boundary conditions for the problem are

$$u'(y,0)=0,\ T(y,0)=T_\infty\ ;\ \ y\geq 0, \quad (3a)$$

$$u'(0,t')=UH(t')cos(\omega' t')\ or\ U\,sin(\omega' t'), \quad (3b)$$

$$\left.\begin{aligned}&T(0,t')=T_\infty+\left(T_w-T_\infty\right)\frac{t'}{t_0},\quad 0<t'\leq t_0,\\&T(0,t')=T_w,\ t'>t_0,\end{aligned}\right\} \quad (3c)$$

$$u'\left(y,t'\right)\to 0,\ T\left(y,t'\right)\to T_\infty\quad as\quad y\to\infty,\ t'\geq 0. \quad (3d)$$

where u' is the velocity components along the x- direction, T is the temperature of the nanofluid, ω' is the frequency of oscillations of the plate, g is the acceleration due to gravity, ρ_{nf} is density of the nanofluid, μ_{nf} is the dynamic viscosity of nanofluid, $(\rho\beta)_{nf}$ is the thermal expansion coefficient of nanofluid, σ_{nf} is the electrical conductivity of nanofluid, $(\rho C_p)_{nf}$ is the heat capacitance of nanofluid and its expressions are given by (Mustafa *et al*., 2016)

$$\mu_{nf}=\mu_f\big/\left(1-\varphi\right)^{2.5},\ \rho_{nf}=\left(1-\varphi\right)\rho_f+\varphi\rho_s,$$

$$\left(\rho C_p\right)_{nf}=\left(1-\varphi\right)\left(\rho C_p\right)_f+\varphi\left(\rho C_p\right)_s,$$

$$\left(\rho\beta\right)_{nf}=\left(1-\phi\right)\left(\rho\beta\right)_f+\phi\left(\rho\beta\right)_s,$$

$$\sigma_{nf}=\sigma_f\left[1+\left\{3\left(\sigma_s-\sigma_f\right)\varphi\right\}\big/\left\{\left(\sigma_s+2\sigma_f\right)-\left(\sigma_s-\sigma_f\right)\varphi\right\}\right],$$

$$\frac{k_{nf}}{k_f}=\left\{\left(k_s+2k_f\right)-2\varphi\left(k_f-k_s\right)\right\}\big/\left\{\left(k_s+2k_f\right)+\varphi\left(k_f-k_s\right)\right\},$$

where ϕ is the solid volume fraction of nanoparticle, μ is the dynamic viscosity, β is thermal expansion coefficient, ρ is the density, σ is the electrical conductivity, k is thermal conductivity. Here, the subscripts nf, f and s represent the thermo-physical properties of the nanofluid, base fluid and the solid nanoparticles respectively.

The thermophysical properties of the base fluid (water), magnetite Fe_3O_4 and non-magnetic Al_2O_3 are provided in Table 1.

In the case of optically thin gray fluid, assuming the temperature differences within the flow sufficiently small, we get

$$\frac{\partial q_r}{\partial y}=-16a^*\sigma^*T_\infty^4\left(T_\infty-T\right), \quad (4)$$

On the use of Eq. (4), Eq. (2) becomes

$$\left(\rho C_p\right)_{nf}\frac{\partial T}{\partial t}=k_{nf}\frac{\partial^2 T}{\partial y^2}-16a^*\sigma^*T_\infty^4\left(T-T_\infty\right), \quad (5)$$

Here t', t_0, σ^*, a^* and $H(.)$ are respectively the time, characteristic time, Stefan- Boltzmann constant, mean absorption coefficient and Heaviside unit step function

Introducing following non-dimensional variables

$$\eta = U\,y/\nu_f\,,\ t = U^2 t'/\nu_f\,,\ u = u'/U\,,$$

$$\theta = (T - T_\infty)/(T_w - T_\infty) \text{ and } t_0 = \upsilon_f/U^2\,, \quad (6)$$

Eqs. (1) and (5), in non-dimensional form, reduce to

$$\frac{\partial u}{\partial t} = E_1 \frac{\partial^2 u}{\partial \eta^2} + E_2\, G_r\, \theta - E_3\, M^2\, u, \quad (7)$$

$$\frac{\partial \theta}{\partial t} = E_4 \frac{\partial^2 \theta}{\partial \eta^2} - E_5\, \theta, \quad (8)$$

where,

$$E_1 = \left(1/(1-\varphi)^{2.5}\right)\left[1/\left((1-\varphi)+\varphi\left(\rho_s/\rho_f\right)\right)\right]$$

$$E_2 = \left[\frac{\left\{(1-\phi)+\phi\left((\rho\beta)_s/(\rho\beta)_f\right)\right\}}{\left\{(1-\varphi)+\varphi\left(\rho_s/\rho_f\right)\right\}}\right],$$

$$E_3 = \left\{\sigma_{nf}/\sigma_f\right\}\left\{1/\left((1-\varphi)+\varphi\left(\rho_s/\rho_f\right)\right)\right\},$$

$$E_4 = \left\{k_{nf}/k_f\right\}\left[1/\left\{P_r\left((1-\phi)+\varphi\left((\rho C_p)_s/(\rho C_p)_f\right)\right)\right\}\right],$$

$$E_5 = \left[N_r/\left\{\Pr\left((1-\phi)+\varphi\left((\rho C_p)_s/(\rho C_p)_f\right)\right)\right\}\right],$$

in which $M^2 = \sigma_f B_0^2 \nu_f/\rho_f U^2$ is the magnetic parameter, $N_r = 16\sigma^* a^* T_\infty^3 \nu_f/k_f U^2$ is the radiation parameter, $\Pr = (\mu C_p)_f/k_f$ is the Prandtl number and $G_r = g\beta\nu_f(T_w - T_\infty)/U^3$ is the Grashof number.

The initial and boundary conditions (3a) to (3d), in non-dimensional form, become

$$u(\eta,0) = 0,\ \theta(\eta,0) = 0, \qquad \eta \geq 0, \quad (9a)$$

$$u(0,t) = H(t)\cos(\omega t) \quad or\ \sin(\omega t), \quad (9b)$$

$$\theta(0,t) = \begin{cases} t, & 0 < t \leq 1 \\ 1, & t > 1 \end{cases} = \theta H(t) - (t-1)H(t-1), \quad (9c)$$

$$u(\eta,t) \to 0,\ \theta(\eta,t) \to 0 \quad \text{as } \eta \to \infty \text{ and } t \geq 0. \quad (9d)$$

where $\omega = \nu_f\,\omega'/U^2$ is the frequency parameter.

III. EXACT SOLUTIONS

In order to find exact solutions of the system of Eqs. (7) and (8), we have used the Laplace transform technique. Thus by taking Laplace transforms of Eqs. (7) and (8) and using initial and boundary conditions (9a) to (9d), we get the solutions for the velocity and temperature field as

$$u_c(\eta,t) = u_1(\eta,\alpha,\gamma_2,\gamma,i\omega,t) + u_1(\eta,\alpha,\gamma_2,\gamma,-i\omega,t)$$
$$+\left\{G_r\delta/\alpha_3\right\}\left\{u_2(\eta,t) - H(t-1)u_2(\eta,t-1)\right\} \quad (10)$$

$$u_s(\eta,t) = i\,u_1(\eta,\alpha,\gamma_2,\gamma,i\omega,t) - i\,u_1(\eta,\alpha,\gamma_2,\gamma,-i\omega,t)$$
$$+\left\{G_r\delta/\alpha_3\right\}\left\{u_2(\eta,t) - H(t-1)u_2(\eta,t-1)\right\}, \quad (11)$$

$$\theta(\eta,t) = f_1(\eta,\alpha_1,\alpha_2,\gamma_3,t)$$
$$-H(t-1)\, f_1(\eta,\alpha_1,\alpha_2,\gamma_3,t-1), \quad (12)$$

where,

$\alpha = 1/E_1$, $\gamma = M^2 E_3/E_1$, $\delta = E_2/E_1$, $\alpha_1 = 1/E_4$, $\alpha_2 = E_5/E_4$, $\alpha_3 = 1/E_4 - 1/E_1$, $\alpha_4 = M^2 E_3/E_1 - E_5/E_4$, $\gamma_1 = \alpha_4/\alpha_3$, $\gamma_2 = \gamma/\alpha$, $\gamma_3 = \alpha_2/\alpha_1$.

Subscripts *c* and *s* correspond to the solutions for cosine and sine oscillations respectively.

IV. SKIN FRICTION COEFFICIENT AND NUSSELT NUMBER

Physical quantities of practical interest are the skin friction τ and Nusselt number *Nu*, which are defined, in non-dimensional form, as

$$\tau = \frac{1}{(1-\phi)^{2.5}}\left(\frac{\partial u}{\partial \eta}\right)_{\eta=0} \quad \text{and} \quad Nu = -\frac{k_{nf}}{k_f}\left(\frac{\partial \theta}{\partial \eta}\right)_{\eta=0}.$$

The expressions of the skin friction and Nusselt number are determined from Eqs. (10) and (12) and are given by

$$\tau(0,t) = \frac{1}{(1-\phi)^{2.5}}\Big[\tau_1(0,\alpha,\gamma,i\omega,t) + \tau_1(0,\alpha,\gamma,-i\omega,t)$$
$$+\left\{G_r\delta/\alpha_3\right\}\left\{\tau_2(0,t) - H(t-1)\tau_2(0,t-1)\right\}\Big], \quad (13)$$

$$Nu = -\left\{k_{nf}/k_f\right\}\Big[Nu_1(0,\alpha_1,\alpha_2,\gamma_3,t)$$
$$-H(t-1)Nu_1(0,\alpha_1,\alpha_2,\gamma_3,t-1)\Big]. \quad (14)$$

V. RESULTS AND DISCUSSION

Numerical results of the present study have been presented for different values of emerging parameters such as magnetic parameter M^2, frequency parameter ω, Grashof number G_r, radiation parameter N_r, time *t* and nanoparticle volume fraction ϕ. We have fixed the values of Prandtl number as Pr=6.2 throughout the study. We can see from the solutions that analytical results are obtained from both cosine and sine oscillations whereas the numerical results are plotted for the velocity only considering cosine oscillations.

Numerical values of fluid velocity $u(\eta,t)$, computed from the solution (10), and fluid temperature $\theta(\eta,t)$,, computed from the solution (12), are presented graphically in the boundary layer region versus boundary layer coordinate η in Figs. 2 to 9.

Figure 2 displays the influence of magnetic field and frequency of oscillations on the velocity profiles of the flow. It is evident from Fig. 2 that both magnetic field and frequency of oscillations have a tendency to reduce the fluid velocity. Physically, it is true because effect of magnetic field gives rise to Lorenz force, which is similar to drag force and causes the fluid to move slowly. Also as ω increases, magnitude of plate oscillation (cosine oscillation) decreases which results in reduction the fluid velocity. The impact of thermal buoyancy force on the fluid velocity is plotted in Fig. 3. It is evident that, velocity of ferrofluid increases with an increase in G_r. Thermal Grashof number G_r signifies the relative influence of thermal buoyancy force to the viscous force in the boundary layer region. For small values of G_r, viscosity dominates and buoyancy dominates when there is a larger value of this parameter. Thus an increase in the values of thermal Grashof number has the tendency to induce much flow in the boundary layer region due to the effect of thermal buoyancy force. Here positive values of G_r represents cooling problem. Moreover, the cooling problem is of great importance and mostly encountered in engineering applications, in the cooling of electronic components and nuclear reactors. Impact of radiation parameter N_r and time t is sketched in Fig. 4. It is revealed from Fig. 4 that thermal radiation has a tendency to decelerate the fluid velocity. From the definition of N_r, when N_r increases, conduction contribution decreases and thermal radiative contribution recedes. Therefore, a lower radiative flux is present for higher values of N_r, and this exerts a decelerating influence on nanofluid boundary layer flow. On the other hand, the velocity enhances with the progress of time. Figure 5 preserves the effects of nanoparticle volume fraction ϕ on the fluid velocity. It is observed from Fig. 5 that an increase in the nanoparticle volume fraction ϕ depreciates the velocity u. Physically, it is true because when the volume fraction of nanoparticles increases in the base fluid, the conductivity and viscosity of the nanofluid increase and cause to slow down the fluid velocity. Figure 6 shows a comparison of velocities when two different types of nanoparticles, namely, magnetite and non-magnetic Al_2O_3 were added to the conventional base fluid. It is found that the velocity of Al_2O_3 nanofluid is greater than that of ferrofluid. This implies that the viscosity and thermal conductivity of the ferrofluid is higher than those of the Al_2O_3 nanofluid. The temperature profiles are depicted in Fig. 7 for different values of N_r and time t. It is found from Fig. 7 that fluid temperature θ decreases on increasing N_r whereas it increases on increasing time t. Figure 8 demonstrates the effect of nanoparticle volume fraction ϕ on the temperature profiles. It is clear from Fig. 8 that unlike the velocity, the temperature increases with the increase in ϕ. This is due to the fact that, increasing the volume fractions results in an increase in the thermal conductivity of the ferrofluid and, therefore, causes the temperature to increase. Figure 9 is plotted for the com- parison of temperature profiles of Al_2O_3 nanofluid and ferrofluid. It is found that the temperature is varied in the same manner as we have noticed in the case of velocity i.e. the temperature of Al_2O_3 nanofluid is higher than that of ferrofluid. It is well known that the thermal conductivity and viscosity of the ferrofluid depend on temperature. With the increase in temperature, thermal conductivity increases whilst viscosity decreases. Numerical values of skin friction τ and Nusselt number Nu, computed from expressions (13) and (14), are presented in tabular form in Tables 2, 3 and 4. It is observed from Tables 2 and 3 that skin friction of ferrofluid and Al_2O_3 nanofluid increases on increasing M^2, N_r and ϕ whereas it decreases with the increase in ω, G_r and t. This implies that the magnetic field, thermal radiation and nanoparticle volume fraction tend to enhance skin friction of both ferrofluid and Al_2O_3 nanofluid whereas frequency of oscillations, thermal buoyancy force and time have reverse effect on it. It is evident from Table 4 that Nu increases on increasing N_r, ϕ and t for both the fluids under consideration. This implies that thermal radiation, nanoparticle volume fraction and time enhance the rate of heat transfer at the plate for both ferrofluid and Al_2O_3 nanofluid.

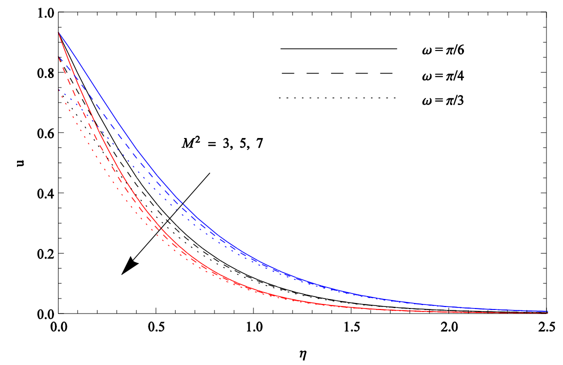

Figure 2: Velocity profiles when G_r=7, N_r=2, t=0.7 and ϕ=0.03.

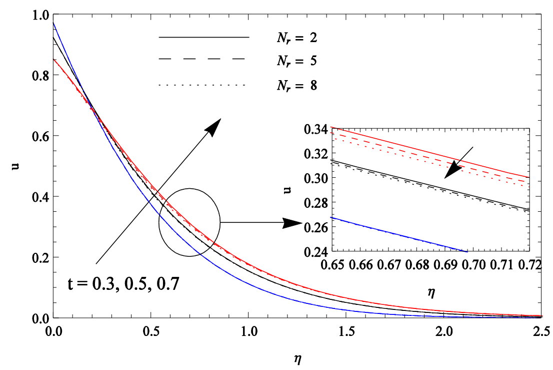

Figure 4: Velocity profiles when M^2=3, ω=π/4, G_r=7 and ϕ=0.03.

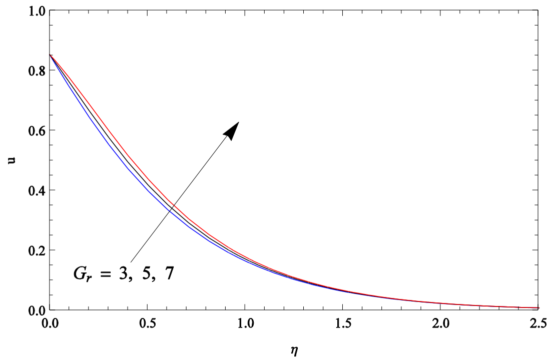

Figure 3: Velocity profiles when M^2=3, ω=π/4, N_r=2, t=0.7 and ϕ=0.03.

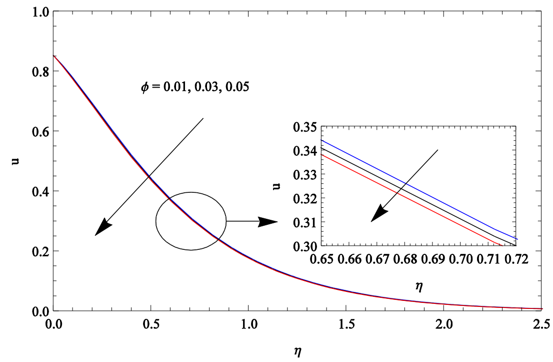

Figure 5: Velocity profiles when M^2=3, ω=π/4, G_r=7, N_r=2 and t=0.7.

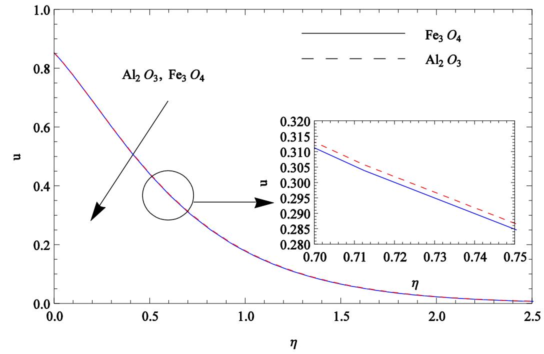

Figure 6: Comparison of velocity profiles when M^2=3, ω=π/4, G_r=7, N_r=2, t=0.7 and ϕ=0.03.

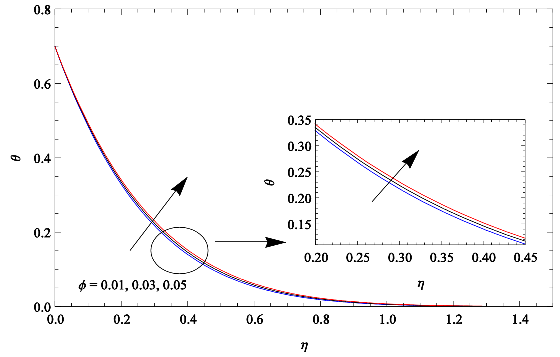

Figure 8: Temperature profiles when N_r=2 and t=0.7.

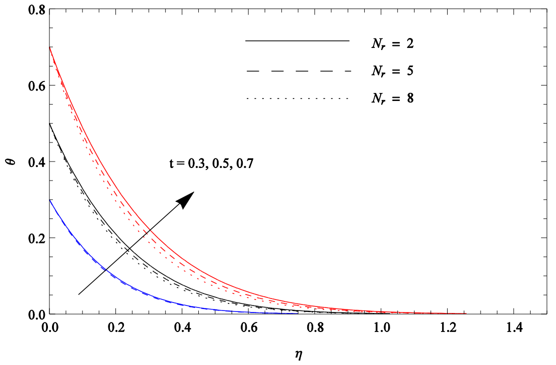

Figure 7: Temperature profiles when ϕ=0.03.

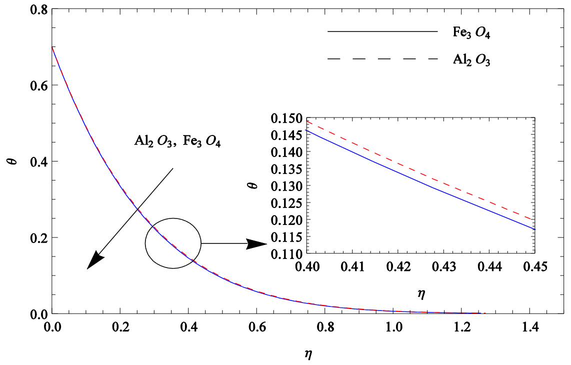

Figure 9: Comparison of temperature profiles when N_r=2, t=0.7 and ϕ=0.03.

Table 2: Skin friction variation when N_r=2, ϕ=0.03 and t=0.7.

M^2	ω	G_r	$-\tau$ (Fe_3O_4)	$-\tau$ (Al_2O_3)
3	$\pi/4$	7	0.729364	0.614273
5	$\pi/4$	7	1.246470	1.096000
7	$\pi/4$	7	1.670130	1.492940
3	$\boldsymbol{\pi/6}$	7	0.945685	0.822104
3	$\boldsymbol{\pi/3}$	7	0.439004	0.335403
3	$\pi/4$	**3**	1.170360	1.062580
3	$\pi/4$	**5**	0.949860	0.838425

Table 3: Skin friction variation when M^2=3, ω=π/4 and G_r=7.

N_r	t	ϕ	$-\tau$ (Fe_3O_4)	$-\tau$ (Al_2O_3)
2	0.7	0.03	0.729364	0.614273
5	0.7	0.03	0.761018	0.646758
8	0.7	0.03	0.789428	0.675899
2	**0.3**	0.03	1.674670	1.568610
2	**0.5**	0.03	1.213120	1.100080
2	0.7	**0.01**	0.648814	0.611183
2	0.7	**0.05**	0.814521	0.618797

Table 4: Nusselt number variation.

N_r	t	ϕ	Nu (Fe_3O_4)	Nu (Al_2O_3)
2	0.7	0.03	2.60339	2.62383
5	0.7	0.03	2.85840	2.88156
8	0.7	0.03	3.09858	3.12426
2	**0.3**	0.03	1.63787	1.65053
2	**0.5**	0.03	2.15764	2.17446
2	0.7	**0.01**	2.55024	2.55703
2	0.7	**0.05**	2.65685	2.69110

VI. CONCLUSIONS

Significant results for the present study are summarized below:

- The effects of magnetic field, thermal radiation, nanoparticle volume fraction and frequency of oscillations on the fluid velocity are opposite to that of thermal buoyancy force and time.
- Fluid temperature attenuates when thermal radiation is intensified but a reverse effect is observed for nanoparticle volume fraction and time.
- The velocity and temperature of magnetite nanofluid are smaller than that of non-magnetic Al_2O_3 nanofluid.
- Magnetic field and thermal radiation tend to enhance the skin friction whereas frequency of oscillations of the plate, thermal buoyancy force and time, have reverse effect on it.
- Thermal radiation and time enhances the rate of heat transfer at the plate.
- Skin friction and Nusselt number are directly proportional to the nanoparticle volume fraction.

ACKNOWLEDGEMENT

Authors are grateful to the reviewers for their valuable suggestions and comments, which helped them to improve the quality of this research paper. One of the authors P. K. Mandal, is thankful to Indian Institute of Technology (Indian School of Mines), Dhanbad to provide research fellowship to carry out this research work.

APPENDIX

$$u_1(\eta,c_1,c_2,c_3,c_4,t)=\left(H(t)/4\right)e^{-c_4 t}\left[e^{\sqrt{(c_2-c_1c_4)}\eta}\times\right.$$

$$erfc\left(\sqrt{(c_3-c_4)t}+\left(\eta\sqrt{c_1}/2\sqrt{t}\right)\right)+e^{-\sqrt{(c_2-c_1c_4)}\eta}\times$$

$$\left.erfc\left(-\sqrt{(c_3-c_4)t}+\left(\eta\sqrt{c_1}/2\sqrt{t}\right)\right)\right],$$

$$u_2(\eta,t)=u_2'(\eta,\alpha,\gamma,\gamma_1,\gamma_2,t)-u_2'(\eta,\alpha_1,\alpha_2,\gamma_1,\gamma_3,t),$$

$$u_2'(\eta,c_5,c_6,c_7,c_8,t)=\left(1/2c_7^{\,2}\right)\left[e^{c_7 t}\left\{e^{\sqrt{(c_7+c_8)c_5}\eta}\times\right.\right.$$

$$erfc\left(\sqrt{(c_7+c_8)t}+\left(\eta\sqrt{c_5}/2\sqrt{t}\right)\right)+e^{-\sqrt{(c_7+c_8)c_5}\eta}\times$$

$$\left.erfc\left(-\sqrt{(c_7+c_8)t}+\left(\eta\sqrt{c_5}/2\sqrt{t}\right)\right)\right\}$$

$$-c_7\left\{e^{\sqrt{c_6}\eta}erfc\left(\sqrt{c_8 t}+\frac{\eta\sqrt{c_5}}{2\sqrt{t}}\right)\times\left(\frac{1}{c_7}+t+\frac{\eta\sqrt{c_5}}{2\sqrt{c_8}}\right)\right.$$

$$\left.\left.+e^{-\sqrt{c_6}\eta}erfc\left(-\sqrt{c_8 t}+\frac{\eta\sqrt{c_5}}{2\sqrt{t}}\right)\left(\frac{1}{c_7}+t-\frac{\eta\sqrt{c_5}}{2\sqrt{c_8}}\right)\right\}\right],$$

$$f_1(\eta,\zeta_1,\zeta_2,\zeta_3,t)=\frac{1}{2}\left[e^{\eta\sqrt{\zeta_2}}erfc\left(\sqrt{\zeta_3 t}+\frac{\eta\sqrt{\zeta_1}}{2\sqrt{t}}\right)\times\right.$$

$$\left.\left(t+\frac{\eta\sqrt{\zeta_1}}{2\sqrt{\zeta_3}}\right)+e^{-\eta\sqrt{\zeta_2}}erfc\left(-\sqrt{\zeta_3 t}+\frac{\eta\sqrt{\zeta_1}}{2\sqrt{t}}\right)\left(t-\frac{\eta\sqrt{\zeta_1}}{2\sqrt{\zeta_3}}\right)\right],$$

$$\tau_1(0,c_{13},c_{14},c_{15},t)=-\frac{H(t)}{2}e^{-tc_{15}}\left\{\frac{e^{\left(-\frac{c_{14}t}{c_{13}}+tc_{15}\right)}\sqrt{c_{13}}}{\sqrt{\pi t}}\right.$$

$$\left.+\sqrt{(c_{14}-c_{13}c_{15})}\,erf\left(\sqrt{\left\{t\left(c_{14}-c_{13}c_{15}\right)/c_{13}\right\}}\right)\right\},$$

$$\tau_2(0,t)=\tau_2'(0,\alpha,\gamma,\gamma_1,\gamma_2,t)-\tau_2'(0,\alpha_1,\alpha_2,\gamma_1,\gamma_3,t),$$

$$\tau_2'(0,c_{16},c_{17},c_{18},c_{19},t)=\frac{1}{2c_{18}}\left\{\frac{2e^{-tc_{19}}\sqrt{c_{16}}\left(t+\frac{1}{c_{18}}\right)}{\sqrt{\pi t}}\right.$$

$$\left.+2\sqrt{c_{17}}erf\left(\sqrt{tc_{19}}\right)\left(t+\frac{1}{c_{18}}\right)+\sqrt{\frac{c_{16}}{c_{19}}}erf\left(\sqrt{tc_{19}}\right)\right\}-\frac{e^{tc_{18}}}{2c_{18}^{\,2}}\times$$

$$\left\{\frac{2e^{-t(c_{18}+c_{19})}\sqrt{c_{16}}}{\sqrt{\pi t}}+2erf\left(\sqrt{t(c_{18}+c_{19})}\right)\sqrt{c_{16}(c_{18}+c_{19})}\right\},$$

$$Nu_1(0,\zeta_4,\zeta_5,\zeta_6,t)=e^{-t\zeta_6}\sqrt{(t\zeta_4/\pi)}$$

$$+\left(t\sqrt{\zeta_5}+\left(\zeta_4/2\sqrt{\zeta_5}\right)\right)erf\left(\sqrt{t\zeta_6}\right).$$

REFERENCES

Adesanya, S.O., E.O. Oluwadare, J.A. Falade and O.D. Makinde, "Hydromagnetic natural convection flow between vertical parallel plates with time-periodic boundary conditions," *J. Magnetsm Magnetic Materials*, **396**, 295-303 (2015).

Beg, O.A., M.M. Rashidi, M. Akbari and A. Hosseini, "Comparative numerical study of single-phase and two-phase models for bio-nanofluid transport phenomena," *J. Mech. In Medicin and Biology*, **14**, 1450011, 31 pages (2014).

Bhatti, M.M and M.M. Rashidi, "Effects of thermo-diffusion and thermal radiation on Williamson nanofluid over a porous shrinking/stretching sheet," *J. Molecular Liquids*, **221**, 567-573 (2016).

Chandran, P., N.C. Sacheti and A.K. Singh, "Natural convection near a vertical plate with ramped wall temperature," *Heat Mass Transf.*, **41**, 459-464 (2005).

Choi, S.U.S., *Enhancing thermal conductivity of fluids with nanoparticle, Developments and Applications of non- Newtonian flows*, D.A. Siginer, H.P. Wang Editions, ASME FED, **231**/MD-**66**, 99-105 (1995).

Das, S. and R.N. Jana, "Natural convective magneo-nanofluid flow and radiative heat transfer past a moving vertical plate," *Alexandria Eng. J.*, **54**, 55-64 (2015).

Das, S., S. Chakraborty, R.N. Jana and O.D. Makinde, "Entropy analysis of unsteady magneto-nanofluid flow past an accelerating stretching sheet with convective boundary conditions," *Appl. Math. Mech.*, **36**, 1593-1610 (2015).

Gul, A., I. Khan, S. Shafie and A. Khalid, "Heat transfer in MHD mixed convection flow of a ferrofluid along a vertical channel," *Plos One*, DOI: 10.1371/Joural Pone. 0141213 (2015).

Jue, T.Ch., "Analysis of combined thermal and magnetic convection ferrofluid flow in a cavity," *Int. Commun. Heat Mass Transf.*, **33**, 846-452 (2006).

Khalid, A., I. Khan and S. Shafie, "Exact solutions for free convection flow of nanofluids with ramped wall temperature," *Eur. Phys. J. Plus*, **130**, Article Id: 57, 14 Pages (2015).

Khamis, S., O.D. Makinde and Y. Nkansah-Gyekye, "Unsteady flow of variable viscosity Cu-water and Al_2O_3-water nanofluids in a porous pipe with buoyancy force," *Int. J. Numer. Methods in Heat Fluid Flow*, **25**, 1638-1657 (2015).

Khan, Z.H., W.A. Khan, M. Qasim and I.A. Shah, "MHD stagnation point ferrofluid flow and heat transfer toward a stretching sheet," *IEEE Trans. Nanotech*., **13**, 35-40 (2014).

Kuznetsov, A.V. and D.A. Nield, "Natural convective boundary-layer flow of a nanofluid past a vertical plate: A revised model," *Int. J. Therm. Sci*., **77**, 126-129 (2014).

Lee, S. and M.M. Yovanovich, "Laminar natural convection from a vertical plate with a step change in wall temperature," *J. Heat Transf.*, **113**, 501-504 (1991).

Moraveji, M.K. and M. Hejazian, "Natural convection in a rectangular enclosure containing an oval-shaped heat source and filled with Fe_3O_4 water nanofluid," *Int. Commun. Heat Mass Transf.*, **44**, 135-146 (2013).

Mustafa, M., A. Mushtaq, T. Hayat and A. Alsaedi, "Rotating flow of magnetite-water nanofluid over a stretching surface inspired by non-linear thermal radiation," *Plos One*, DOI: 10.1371/Joural Pone. 0149304 (2016).

Mutuku-Njane, W.N. and O.D. Makinde, “On hydromagnetic boundary layer flow of nanofluids over a permeable moving surface with Newtonian heating,” *Latin American Appl. Res*., **44**, 57-62 (2014).

Nandkeolyar, R., M. Das and H. Pattnayak, “Unsteady hydromagnetic radiative flow of a nanofluid past a flat plate with ramped temperature,” *J. Orissa Math. Soc*., **32**, 15-30 (2013).

Rashidi, M.M., M. Nasiri, M. Khezerloo and N. Laraqi, “Numerical investigation of magnetic field effect on mixed convection heat transfer of nanofluid in a channel with sinusoidal walls,” *J. Magnetsm Magnetic Materials*, **401**, 159-168 (2016).

Schetz, J.A., “On the approximate solution of viscous-flow problems,” *J. Appl. Mech*. **30**, 263-268 (1963).

Seth G.S., Md.S. Ansari and R. Nandkeolyar, “MHD natural convection flow with radiative heat transfer past an impulsively moving plate with ramped wall temperature,” *Heat Mass Transfer*, **47**, 551-561 (2011).

Sheikholeslami, M. and D.D. Ganji, “Ferrohydrodynamic and magnetohydrodynamic effects on ferrofluid flow and convective heat transfer,” *Energy*, **75**, 400-410 (2014).

Sheikholeslami, M., M. Gorji Bandpy and D.D. Ganji, “Numerical investigation of MHD effects on Al_2O_3–water nanofluid flow and heat transfer in a semi-annulus enclosure using LBM,” *Energy*, **60**, 501-510 (2013).

Sheikholeslami, M., M. Hatami and D.D. Ganji, “Nanofluid flow and heat transfer in a rotating system in the presence of a magnetic field,” *J. Molecular Liquids*, **190**, 112-120 (2014).

Sheikholeslami, M., M.M. Rashidi and D.D. Ganji, “Effect of non-uniform magnetic field on forced convection heat transfer of Fe_3O_4-water nanofluid,” *Comp. Methods in Appl. Mech. Eng*., **294**, 299-312 (2015).

Received: December 15, 2016.
Sent to Subject Editor: February 17, 2017.
Accepted: July 17, 2017.
Recommended by Subject Editor: Gianfranco Caruso